Scientific Research Publishing

International Journal of Geosciences, 2025, 16(2), 127-153
https://www.scirp.org/journal/ijg
ISSN Online: 2156-8367
ISSN Print: 2156-8359

Geochemical Characterizations of the Hypovolcanic Formations of the Pan-African Basement and the Cretaceous Sedimentary Basins of Figuil (North Cameroon) and Léré (South-West Chad): Petrogenetic and Geodynamic Implication of the Pan-African Range of Central Africa (CPAC)

Klamadji Moussa Ngarena[1*], Tekoum Léotine[2], Baïssemia Ronang Gustave[1], Merlin Gountié Dedzo[3], Djérossem Nenadji Felix[4], Béninga Léopold Felix[5], Didi Djamilatou[3]

[1]Department of Mining and Geology Engineering, Faculty of Earth and Life Sciences, University of Pala, Pala, Chad
[2]Department of Geology, Faculty of Exact and Applied Sciences, University of N'Djamena, N'Djamena, Chad
[3]Department of Life and Earth Sciences, High University of Teacher Training, University of Maroua, Maroua, Cameroon
[4]Department of Mines, New and Renewable Energies, National Higher Institute of the Sahara and Sahel, Iriba, Chad
[5]Department of Earth and Universe Sciences, University of Doba, Doba, Chad
Email: *klamadjimoussa@yahoo.fr

How to cite this paper: Ngarena, K.M., Léotine, T., Gustave, B.R., Dedzo, M.G., Felix, D.N., Felix, B.L. and Djamilatou, D. (2025) Geochemical Characterizations of the Hypovolcanic Formations of the Pan-African Basement and the Cretaceous Sedimentary Basins of Figuil (North Cameroon) and Léré (South-West Chad): Petrogenetic and Geodynamic Implication of the Pan-African Range of Central Africa (CPAC). *International Journal of Geosciences*, **16**, 127-153.
https://doi.org/10.4236/ijg.2025.162007

Received: December 12, 2024
Accepted: February 25, 2025
Published: February 28, 2025

Abstract

The study area located between Figuil (Northern Cameroon) and Léré (Southwest Chad) belongs to the northern domain of the Pan-African Range of Central Africa (CPAC). The aim of this work is to highlight the petrogenesis of the hypovolcanic formations affecting the Pan-African base and the Cretaceous sedimentary basins of the study area as well as their geodynamic context. Hypovolcanic formations have a strong affinity with rocks of the continental tholeiitic series. The tholeiitic character with alkaline affinity constitutes the transition between alkaline and tholeiitic magmatisms. The low Rb/Sr ratios (0.24 - 1.24) constitute proof that the dolerites studied do not come from the partial fusion of Pan-African granitoids (Rb/Sr: 2.54 - 7.64) but rather from a mantle source as shown by the similar ratios of Zr/Hf (37.56 - 43.08), Nb/Ta (15.16 - 19.60) of dolerites from the Pan-African basement (DSP) and Zr/Hf (34.34 - 46.48), Nb/Ta (14.34 - 19.3) from dolerites from the Cretaceous sedimentary basins (DBSC). The enrichment in LREE relative to the HREE of the dolerites studied associated with the ratios $(Tb/Yb)_N$ (1.95 - 2.56), Dy/Yb (2.33 - 2.85) characterizes a mantle source of lherzolite with garnet.

Keywords

Hypovolcanic Formations, Geochemistry, Continental Tholeiite, Pan-African Basement, Cretaceous Sedimentary Basin and Figuil-Léré

1. Introduction

Intrusive magmatism generally exploits synchronous fracturing systems and can also follow regenerated pre-existing systems that exhibit network organizations

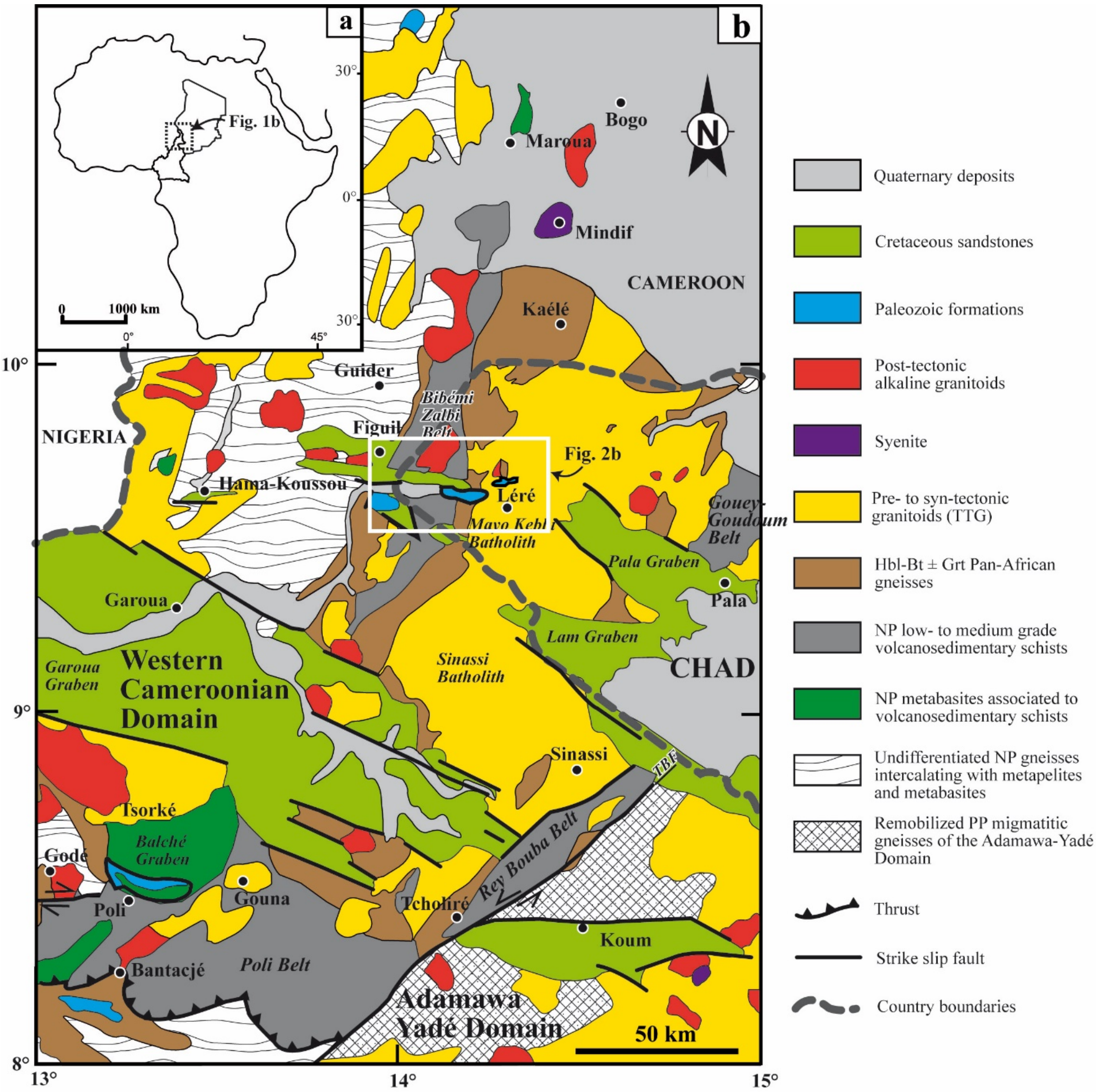

Figure 1. Location of the study area (white rectangle) in the geological map of North Cameroon and South-West Chad (b). In box Cameroon and Chad in Africa (a) [3]. The Cretaceous sediments were emplaced in the two basins (Mayo Oulo-Léré and Babouri-Figuil) limited by major Pan-African faults oriented E-W, whose replay in extension, at the beginning of the Cretaceous, controlled the facies and thicknesses of the continental Cretaceous sediments as well as the establishment of veins and sills [4] [5].

[1]. The study area which is located between Figuil (Northern Cameroon) and Léré (Southwest Chad) belongs to the northern domain of the Pan-African Range of Central Africa (CPAC).

The systematic study of volcanic inclusions, particularly dolerite dikes, would have been of great interest in the understanding of geological phenomena, especially the understanding of Precambrian terrains [2].

The objective of this study is to highlight the petrogenesis of the hypovolcanic formations affecting the Pan-African basement and the Cretaceous sedimentary basins of the study area as well as their geodynamic context of establishment. The half-grabens underwent subsidence (Upper Hauterivian-Lower Aptian), followed by post-rift transpression which affected the entire Senonian fold belt. The study area which includes the Pan-African basement and the Cretaceous sedimentary basins (Mayo Oulo-Léré and Babouri-Figuil and the volcanic veins (dykes) belongs to the Pan-African Range of Central Africa (CPAC) (**Figure 1**). The approach of this study is therefore entirely suitable for providing new data on the geodynamic context of dyke installation and the magmatic activity of the study area.

2. Geological Setting

The Pan-African Range of Central Africa (CPAC), identified in the early 1960s, is a vast geological unit located north of the Congo craton [6]. It extends from the Central African Republic (CAR) to eastern Nigeria via Chad and Cameroon. And, it extends on the other side of the Atlantic, in the province of Borborema, in the North-East of Brazil [7] [8].

2.1. Pan-African Base of Figuil and Léré

The mafic magmatic rocks of Figuil and Léré crossed a basement of middle to upper Proterozoic age, covered by sediments of Lower Cretaceous age [9]. The bedrock of Mayo Kebbi, which extends from Poli in Cameroon to southwest Chad, is interpreted as a Neoproterozoic middle arc, stabilized around 640 Ma [10]. The base of this region is made up of granites and gneisses, which were folded NNE-SSW by the Pan-African orogeny and characterized by the presence of foliations oriented N-S to NNE-SSW carrying an E-W stretching lineation with dips greater than 50˚ towards the West [10]. The base of the Léré basin belongs to the large group known as the Mayo Kebbi region. This set represents the NE extension of the Pan-African base of Poli in North Central Cameroon [10]. It is an assemblage consisting of a Phanerozoic sedimentary platform which covers a Precambrian substratum dominated by the tonalitic batholith intrusive in medium to high grade amphibolic gneissic complexes [11].

Cretaceous Sedimentary Basins of Figuil and Léré

The Mayo Oulo-Léré basin is a half-graben with an asymmetrical syncline structure belonging to the northern Cameroonian intracontinental basins [12]. It is made up of other small sedimentary basins (Babouri-Figuil, Hama-koussou and Koum) with facies from the Lower Cretaceous whose history is linked to the establishment of the Bénoué ditch. The main geological units of the area include the Precambrian basement dated from the Meso to Neoproterozoics between −700 to −1000 Ma [13]; a thick sedimentary pile dated to the Lower Cretaceous which rests unconformably on the Precambrian basement and post-Pan-African magmatic occurrences [14].

The crystalline base of Babouri-Figuil is covered by a thick sedimentary series of approximately 1500 m [15]. Several types of facies (conglomeratic sandstones, coarse sandstones, marly shales, clay shales, sandstone with calcareous cements) and a diversity of sedimentary structures (ripple mark, mark, load structure, channels, sliding structures, convoluted beds, olistolite) were highlighted.

The veins of the Mayo Oulo-Léré basin, from one to twenty meters thick, can be followed in the field, sometimes with a few interruptions, over a total distance of approximately 45 km. They are made up of basalts, fine-grained gabbros and dolerites. The Babouri-Figuil veins (12 km long, 1 to 20 m thick) are made up of camptonites and benmoreites.

3. Material and Methods

3.1. Material

Twenty (20) fresh and representative samples from two groups of dolerites were selected for the geochemical study.

Each sample was carefully cleaned and then sawn into rock sugar tiles. These sugars were sent to Vancouver in Canada, to the "Acme Analytical Laboratories LTD" laboratory, for geochemical analyses.

3.2. Methods

To try to best resolve the problems posed by hypovolcanic formations, the following methodological approach was adopted. A geochemical study was based on the analogy between the observed facts (contents, trends and developments) and theoretical models reflecting the various natural processes. Thus, it was possible to elucidate the conditions of magmatogenesis of the formations studied. This analysis was carried out both at the level of major elements and trace elements:

- ✓ for major elements, a comprehensive major element analysis was carried out by combining a number of methods in a single package. This package combines the entire whole rock analysis package (ME-ICP06) in addition to carbon and sulfur for which a combustion furnace is used (ME-IR08). The major elements as: SiO_2, Al_2O_3, Fe_2O_3, CaO, MgO, Na_2O, K_2O, Cr_2O_3, TiO_2, MnO, P_2O_5, SrO and BaO were analyzed by ICP-AES;
- ✓ on the other hand, plasma source mass spectrometry (Inductively Coupled Plasma-Mass Spectrometry, ICP-MS) was used to examine rare earths as: La, Ce, Pr, Nd, Sm, Eu, Gd, Tb, Dy, Ho, Er, Tm, Yb and Lu, and for Zr, Hf, Y, Cs, Rb, Th, U, Nb and Ta.

4. Results

4.1. Geochemical Characterization

4.1.1. Nomenclature of the Hypovolcanic Formations of Figuil and Léré

Twenty (20) samples of hypovolcanic formations were selected for geochemical analyzes on the basis of their mineralogical and textural homogeneity, their representativeness in outcrop areas and their geographical distribution. Geographically, thirteen samples concern the Léré zone and seven, the Figuil zone. They are distributed as follows in Table 1.

Table 1. Summary of samples analyzed by petrographic type.

Groups	Petrographic type	Locality (Samples analyzed)
Group of dolerites from the Pan-African basement (DSP): ultramafic to mafic dolerites (only one which is intermediate: PletM2)	Pyrite and calcite dolerites	Health school (TESM4) Regional school (TERM4), School of Computer Science (TEIM3) Lampagame (TLM3)
	Pyrite and basement enclave dolerites	Berliang (BeM3)
	Amphibole and titanite dolerites	Poubamé (PmeM2), Poutalet (PletM2) And Zabili (ZiM3
	Pyrite dolerites	input (FefM1) Figuil city center (FcvM1)
Group of dolerites from the Pan-African basement DBSC: mafic to intermediate dolerites (single acid and differentiated: FsmM1)	Amphibole dolerites	Dissing (DiM3)
	Biotite and pyroxene dolerites	Zalbi (ZaM1), Teuchéné (T2M, T2M3) and Djalingo (DjM3)
	Pyroxene dolerites	Tchontchi Golombé (FtgM3
	Fine-grained Gabbros	Bissoli (FbiM1 and FbiM2) Badadji (FbaM1)
	Trachytes	Mayo-Sorowel (FmsM1)

4.1.2. Geochemical Characterization of Hypovolcanic Rocks of the Pan-African Basement

The whole rock geochemical analysis data of the hypovolcanic rock samples from the Pan-African basement are reported in Table 2. With the exception of one sample (PletM2 which is a trachy-andesite), all the rocks have a basaltic composition with a homogeneous chemical composition: 43.85% < SiO_2 < 48.67%; 11.91 < Fe_2O_3 < 16.83%; 4.04 < MgO < 7.58%; 2.12 < TiO_2 < 3.44%; 14.5 < Al_2O_3 < 16.18%; $Na_2O + K_2O \approx 4\%$.

Table 2. Whole rock analyzes of dolerite dikes outcropping on the granite bedrock.

Echantillon	TESM4	TEIM3	TERM4	TLM3	BeM3	ZiM2	PmeM2	PletM2	FefM1	Fcv1
Wt %										
SiO_2	45.7	45.87	45.97	44.09	46.05	46.45	48.28	55.87	43.85	48.67
TiO_2	3.44	3.1	2.55	3.03	3.32	2.12	2.16	1.28	2.47	2.82
Al_2O_3	14.71	15.03	15.69	14.65	14.5	16.18	15.7	14.82	14.51	14.82

Continued

Fe_2O_3	15.64	15.39	13.76	15.15	16.83	11.91	12.34	7.13	12.73	12.09
MnO	0.18	0.19	0.17	0.18	0.2	0.18	0.19	0.1	0.17	0.14
MgO	4.68	4.34	4.96	4.41	4.07	7.41	6.33	5.3	7.58	6.48
CaO	7.23	6.72	6.87	6.87	6.04	9.05	8.41	5.21	10.16	7.76
Na_2O	3.02	3.74	3.5	3.16	3.55	3.01	3.27	4.1	2.68	3.2
K_2O	1.94	1.26	1.38	1.16	1.31	1.04	0.87	3.53	1.37	1.08
P_2O_5	0.59	0.58	0.41	0.55	0.71	0.37	0.38	0.49	0.35	0.34
Cr_2CO_3	<0.002	<0.002	0.002	0.002	0.003	0.022	0.01	0.038	0.023	0.026
P.A.F.	2.5	3.4	4.4	6.4	3.1	2	1.8	1.7	3.7	2.2
Total	99.69	99.71	99.73	99.71	99.71	99.73	99.75	99.73	99.69	99.7
Mg#	**40.2**	**38.8**	**40.2**	**39.5**	**35.5**	**58.3**	**53.5**	**62.6**	**57.2**	**54.6**
Traces (ppm)										
Sc	18.0	17.0	17.0	16.0	14.0	27.0	26.0	13.0	24.0	18.0
Be	1.0	3.0	2.0	6.0	2.0	<1	<1	2.0	<1	3.0
V	272.0	200.0	189.0	204.0	221.0	225.0	218.0	133.0	291.0	260.0
Co	50.9	45.7	47.4	48.6	49.2	46.6	43.8	26.3	50.1	45.1
Ni	38.0	38.0	50.0	33.0	43.0	91.0	62.0	114.0	97.0	107.0
Ga	23.1	22.8	21.0	25.8	22.6	17.2	19.3	18.2	19.8	19.6
Rb	37.6	21.1	23.6	18.4	18.3	29.4	11.9	99.0	18.9	21.5
Sr	593.0	569.7	621.5	677.6	515.3	363.3	366.5	564.3	585.7	679.4
Y	33.2	34.4	25.7	32.9	40.8	28.8	35.2	18.1	18.9	17.3
Zr	298.0	290.1	223.4	280.0	391.4	177.8	201.4	271.5	170.5	172.8
Nb	30.9	27.1	21.4	26.8	35.8	8.5	9.8	13.2	26.6	9.1
Sn	2.0	2.0	2.0	2.0	3.0	1.0	1.0	1.0	2.0	1.0
Cs	1.2	2.4	0.9	7.7	0.4	0.5	0.2	0.7	0.4	0.7
Ba	674.0	653.0	463.0	449.0	613.0	199.0	210.0	972.0	373.0	428.0
La	41.0	36.3	26.7	36.3	44.2	13.2	16.0	50.0	21.3	25.8
Ce	90.5	81.8	60.3	76.9	100.1	33.6	40.4	97.8	45.2	54.2
Pr	11.2	10.5	7.5	9.9	12.3	4.7	5.5	11.3	5.4	6.7
Nd	46.7	42.3	31.9	41.5	51.4	21.7	24.9	44.3	23.6	27.9
Sm	9.4	8.9	6.7	9.2	10.5	5.6	6.1	7.5	5.0	5.9
Eu	2.8	2.7	2,1	2.6	3.1	1.9	2.1	1.9	1.7	2.0
Gd	9.3	9.1	6.7	8.6	10.5	6.0	6.8	6.1	5.2	5.6
Tb	1.2	1.3	1.0	1.2	1.5	1.0	1.1	0.8	0.8	0.7
Dy	7.1	7.1	5.0	7.0	8.4	5.5	6.3	3.6	4.1	3.7
Ho	1.3	1.3	1.0	1.3	1.5	1.1	1.4	0.6	0.8	0.7
Er	3.4	3.6	2.7	3.3	4.3	3.0	3.7	1.7	2.0	1.7
Tm	0.5	0.5	0.3	0.4	0.6	0.4	0.5	0.2	0.3	0.2
Yb	2.8	2.8	2.2	2.7	3.5	2.8	3.4	1.3	1.7	1.3

Continued

Lu	0.4	0.6	0.3	0.4	0.5	0.4	0.5	0.2	0.2	0.2
Hf	7.2	7.0	5.6	6.5	9.2	4.2	4.9	6.4	4.1	4.6
Ta	1.8	1.5	1.2	1.5	2.2	0.5	0.5	0.6	1.7	0.6
W	0.7	<0.5	0.8	1.2	<0.5	0.5	<0.5	1.4	<0.5	<0.5
Th	3.0	2.4	2.1	1.9	3.2	0.6	1.0	7.6	1.7	3.6
U	0.7	0.6	0.7	0.6	0.8	0.3	0.5	1.5	0.6	0.7

The rocks studied are divided into four petrographic subgroups: 1) dolerites with calcite and pyrite, 2) dolerites with pyrite and enclaves rich in alkali feldspars, 3) dolerites with amphibole and titanite and 4) pyrite dolerites. The samples analyzed were mainly tholeiites. The transition element contents of dolerites (Ni: 38 - 114 ppm, Co: 26.30 - 50.90 ppm and V: 133 - 272 ppm) are low compared to the values of magmas typical of the primitive mantle, for example, Ni (250 - 350 ppm) and Co (50 - 70 ppm) [16].

4.1.3. Geochemical Characterization of Hypovolcanic Rocks from Cretaceous Sedimentary Basins

Geochemical analyzes of dolerite, microgabbros and trachyte samples from the Cretaceous sedimentary basin are reported in Table 3.

The chemical composition is relatively homogeneous: dolerites: 48.25% < SiO_2 < 52.59%; 2.73% < $Na_2O + K_2O$ < 4.86%; 10.62 < Fe_2O_3 < 12.09%; 5.40% < MgO < 6.95%; 1.67% < TiO_2 < 2.63%; 14% < Al_2O_3 < 14.72%; microgabbros: 50.19% < SiO_2 < 51.09%; 3.12% < $Na_2O + K_2O$ < 4.04%; 10.92 < Fe_2O_3 < 11.69%; 6.07% < MgO < 7.9%; 1.61% < TiO_2 < 1.91%; 13.7% < Al_2O_3 < 14.1%; trachyte: SiO_2 ≈ 62.05%; 2.73% < $Na_2O + K_2O$ < 4.86%; Fe_2O_3 ≈ 4.23%; MgO ≈ 1.8%; TiO_2 ≈ 0.84%; Al_2O_3 ≈ 16.74%.

Table 3. Analyzes on total rocks (composition in major and trace elements) of dikes outcropping in the sedimentary bedrock.

	DiM3	ZaM1	T2M3	T2M1	DjM2	FtgM3	FbiM1	FbaM1	FbiM2	FmsM1
Wt %										
SiO_2	48.25	49.8	50.01	52.59	49.95	51.79	50.19	50.24	51.09	62.05
TiO_2	2.63	1.67	1.76	1.71	1.86	1.96	1.69	1.91	1.61	0.84
Al_2O_3	14.44	14.36	14.16	14.72	14.62	14	14.1	13.95	13.7	16.74
Fe_2O_3	12.05	11.11	11.22	10.62	10.68	11.49	11.69	10.92	10.97	4.23
MnO	0.16	0.14	0.15	0.14	0.15	0.15	0.15	0.15	0.15	0.05
MgO	6.82	6.95	6.89	5.4	6.04	6.45	7.25	6.07	7.9	1.8
CaO	8.97	9.26	9.24	8.9	9.84	8.38	8.15	9.7	8.97	2.44
Na_2O	3.66	2.43	2.64	3.34	2.49	3.06	3.65	2.68	2.79	5.97
K_2O	1.2	0.3	0.32	0.59	0.37	0.48	0.39	0.44	0.34	3.61
P_2O_5	0.52	0.15	0.15	0.17	0.16	0.19	0.12	0.16	0.14	0.38

Continued

Cr_2CO_3	0.029	0.036	0.039	0.012	0.012	0.036	0.037	0.017	0.053	0.005
P.A.F.	0.9	3.5	3.2	1.6	3.6	1.7	2.3	3.5	2	1.5
Total	99.69	99.77	99.77	99.79	99.78	99.76	99.78	99.77	99.75	99.7
Mg#	**40.2**	**38.8**	**40.2**	**39.5**	**35.5**	**58.3**	**53.5**	**62.6**	**57.2**	**54.6**
Traces (ppm)										
Sc	18.0	20.0	21.0	22.0	24.0	21.0	21.0	24.0	23.0	4.0
Be	3.0	<1	<1	<1	2.0	1.0	<1	<1	<1	5.0
V	190.0	168.0	178.0	196.0	199.0	171.0	179.0	211.0	178.0	36.0
Co	43.5	40.3	39.7	33.1	35.8	37.3	42.2	37.9	42.3	10.1
Ni	94.0	122.0	119.0	50.0	54.0	121.0	136.0	55.0	135.0	30.0
Ga	19.8	17.6	17.2	20.3	18.3	19.3	17.2	17.1	16.5	25.2
Rb	20.3	6.3	6.3	11.0	7.2	8.1	7.5	9.6	6.7	70.2
Sr	761.8	342.9	379.1	301.5	313.9	325.9	285.8	441.9	382.2	1099.1
Y	20.9	17.4	17.4	20.8	17.7	22.2	17.0	18.5	16.8	10.0
Zr	179.9	81.9	79.0	119.0	85.1	119.6	79.0	91.4	79.7	557.8
Nb	36.7	7.3	7.3	10.9	9.5	8.4	6.9	9.4	7.0	50.2
Sn	1.0	<1	<1	<1	<1	<1	<1	<1	<1	1.0
Cs	0.5	0.3	0.1	<0.1	<0.1	0.2	0.2	0.3	0.2	0.5
Ba	498.0	81.0	72.0	119.0	84.0	185.0	73.0	91.0	76.0	708.0
La	24.2	6.5	6.5	10.7	7.6	9.2	5.8	8.5	6.1	55.2
Ce	48.9	14.7	14.4	22.5	17.0	19.9	13.3	18.3	14.0	99.1
Pr	6.0	2.1	2.0	2.9	2.3	2.7	1.9	2.4	2.0	9.9
Nd	26.1	9.5	9.4	13.9	10.9	13.5	8.9	10.7	10.3	32.8
Sm	6.1	2.9	3.0	3.6	3.0	3.9	2.9	3.4	3.0	5.5
Eu	2.2	1.2	1.2	1.4	1.3	1.5	1.1	1.4	1.2	1.7
Gd	6.3	3.9	4.0	4.9	4.1	5.1	3.6	4.2	3.9	4.1
Tb	0.9	0.6	0.6	0.7	0.6	0.8	0.6	0.7	0.6	0.5
Dy	4.7	3.7	3.5	4.3	3.6	4.4	3.5	4.0	3.6	2.1
Ho	0.8	0.7	0.7	0.8	0.7	0.8	0.7	0.8	0.7	0.3
Er	2.1	1.9	1.8	2.2	1.9	2.4	1.8	1.9	1.9	0.8
Tm	0.3	0.2	0.2	0.3	0.2	0.3	0.2	0.2	0.2	0.1
Yb	1.6	1.4	1.4	1.7	1.4	1.9	1.4	1.5	1.4	0.6
Lu	0.2	0.2	0.2	0.3	0.2	0.3	0.2	0.2	0.2	0.1
Hf	4.3	2.3	2.3	3.0	2.3	3.1	2.2	2.5	2.2	12.0
Ta	1.9	0.5	0.4	0.6	0.5	0.5	0.4	0.6	0.4	3.5
W	0.7	<0.5	0.6	<0.5	<0.5	0.6	<0.5	1.1	<0.5	1.4
Th	2.8	0.7	0.6	1.0	0.8	0.8	0.7	0.8	0.7	9.9
U	0.9	0.2	0.2	0.3	0.2	0.2	0.2	0.2	0.2	2.9

The chemical compositions of the different mafic hypovolcanic rocks are projected into the different rock classification diagrams (**Figure 2(a)**) for their characterization. In the TAS diagram (($Na_2O + K_2O$) = f(SiO_2)), the DSPs are plotted in the domains of basanite tephrites and basalts, whereas the DBSCs are placed at the same time in the domains of basalts and andesitic basalts, except the PletM2 and FmsM1 samples which are placed respectively in the trachy-andesite and trachyte ranges. In this diagram, the DSP dolerites are placed in the alkaline field, whereas the DBSC dolerites occupy the sub-alkaline zone (**Figure 2(a)**).

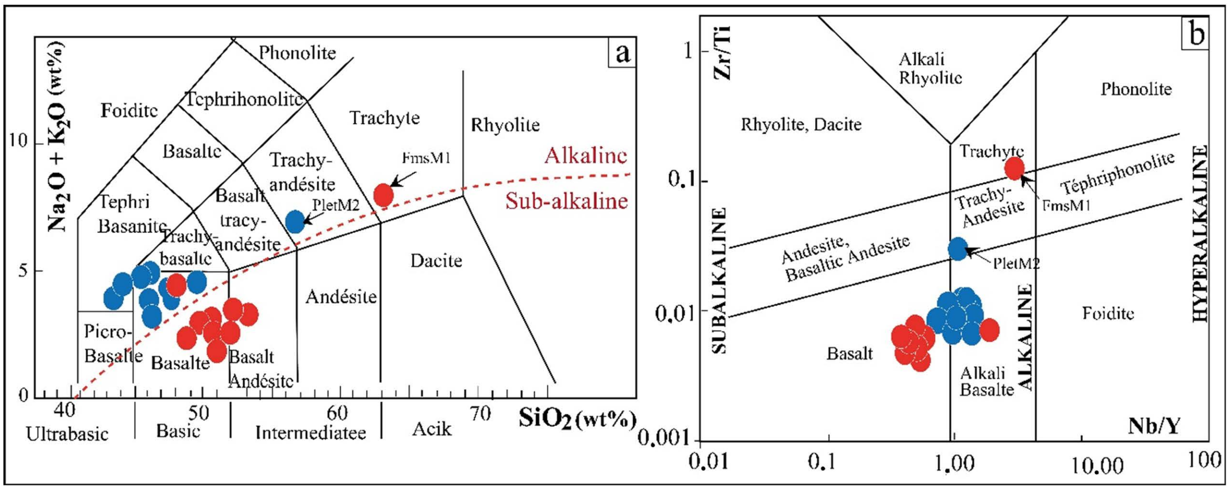

Figure 2. Diagrams showing the classification of mafic hypovolcanic rocks and their hyperaluminosity index. (a) Hypovolcanic formations of Léré-Figuil are plotted in the TAS diagram (Total alkalis vs Silica; Le Bas *et al.* [17]; Le Maitre, [18]). The broken red line separates the alkaline domain from the sub-alkaline domain according to Miyashiro [19], (b) Diagram by Winchester *et al.* [20]) supporting the classification of mafic magmatic rocks studied (modified by Pearce [21]. Figured blue: dolerites from the Pan-African basement (DSP) and Figured red: dolerites from the Cretaceous sedimentary basins (DBSC).

In the Nb/Y vs Zr/Ti diagram of Pearce [21] (**Figure 2(b)**), the classification of rocks is based on trace elements. The vast majority of DSP and DBSC are plotted in the subalkaline basalt domain and two (DSP and DBSC) samples are in the alkaline basalt domain. Except for the PletM2 and FmsM1 samples which are respectively placed in the trachy-andesite and trachyte ranges in the alkaline rock field.

In the TiO_2 vs Y/Nb diagram of Floyd and Winchester [22] (**Figure 3(a)**), most of the rocks are located in the continental tholeiite field. On the other hand, a sample (PletM2) of DSPs is found in the domain of MORBs. Furthermore, one sample (DiM3) of the DBSCs and 2 samples of the DSPs occupy the alkaline range. In the variation diagram of Zr/P_2O_5 * 10,000 vs Nb/Y, the majority of the dolerite samples from Figuil and Léré occupies the range of the tholeiitic series (**Figure 3(b)**). We note that three samples already mentioned above which belonged to the domain of alkaline rocks are still placed in the domain of the alkaline series.

The tholeiitic nature of the studied dolerites appears clearly in the AFM diagram (**Figure 3(c)**), except for the three DSP samples which are located in the calc-alkaline series. The concentration of the samples on the AFM diagram suggests that the alkaline elements are not very disturbed by secondary transformations.

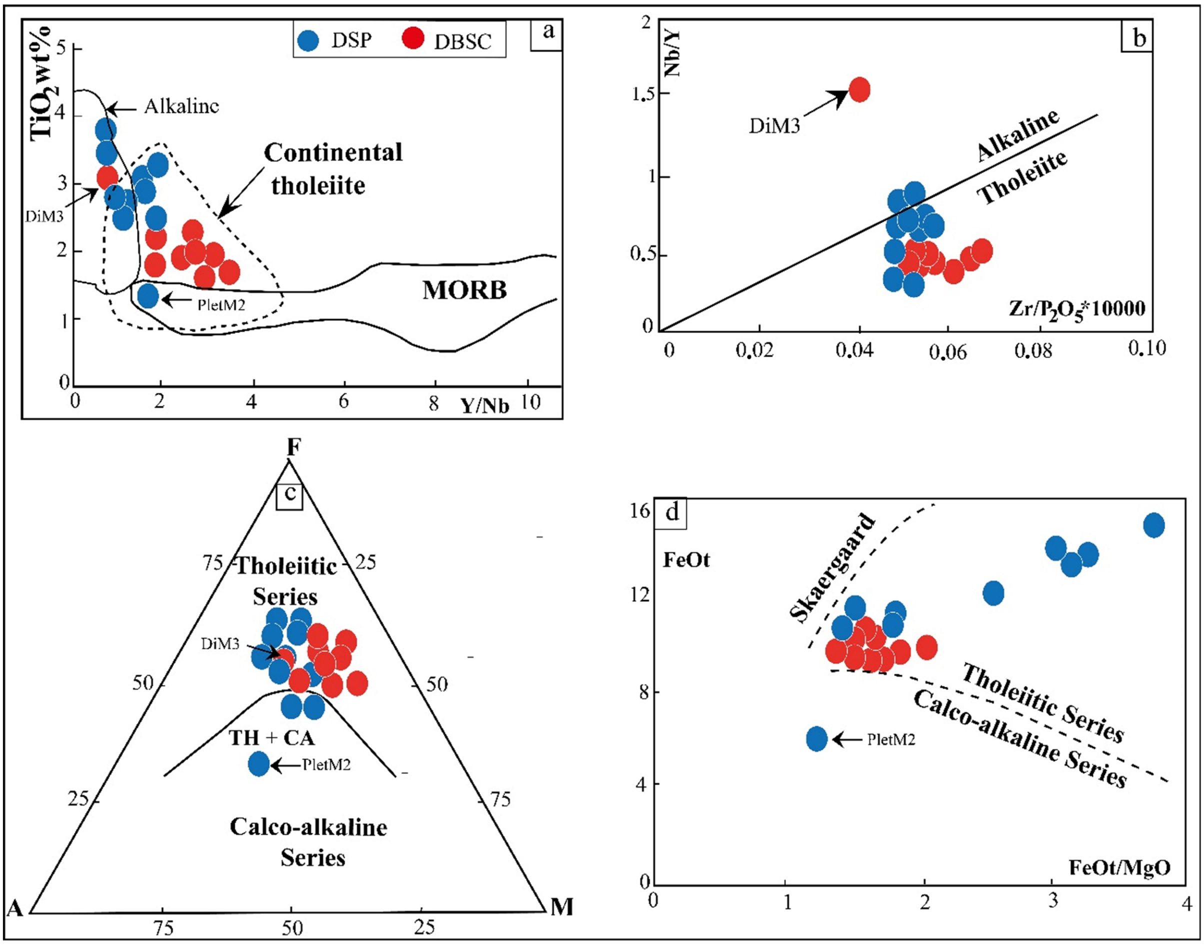

Figure 3. Diagrams illustrating the tholeiitic series of the hypovolcanic formations of Figuil and Léré. (a) TiO_2 vs Y/Nb discrimination diagram from Floyd and Winchester [22], showing the situation of two groups of rocks from the Léré-Figuil sector in the field of continental tholeiites, (b) Variation diagram of Zr/P_2O_5 * 10,000 vs Nb/Y revealing the transitional character of the magmatic series, (c) TiO_2-K_2O-P_2O_5 triangular diagram of Pearce *et al.* [23] applied to the two groups of mafic magmatic rocks of Léré-Figuil. Figured blue: dolerites from the Pan-African basement (DSP) and figured red: dolerites from the Cretaceous sedimentary basins (DBSC).

The tholeiitic nature of these studied dolerites is also illustrated by the FeOt vs (FeOt/MgO) diagram (**Figure 3(d)**). The TiO_2 vs FeOt/MgO diagram [24] suggests that almost all of the rocks in the study area fall into the domain of rocks with high Ti contents (**Figure 3(d)**). We notice in this diagram that the DSPs are richer in titanium oxides than the DBSCs, except for a sample of the DSPs (PletM2) which is placed in the range of low Ti contents. On the other hand, a sample of DBSCs (FmsM1) is found outside two titanium domains.

4.1.4. Behaviors of Elements in Harker Diagrams

✓ **Behavior of major elements**

The Harker diagrams of major elements highlight the evolution of the major elements expressed as a percentage by weight of oxides as a function of SiO_2. These diagrams (**Figure 4**) show a generally linear evolution for most of the major elements.

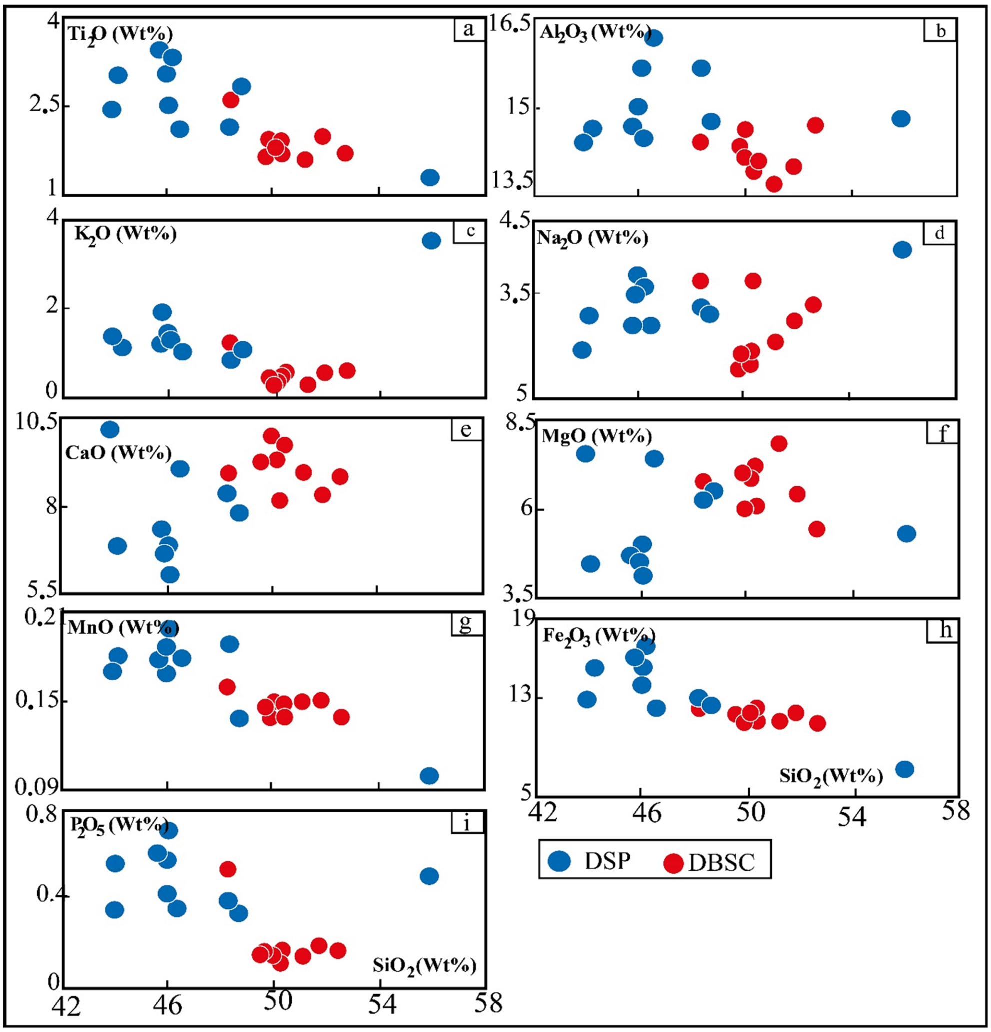

Figure 4. Harker type evolution diagrams showing the variation of major elements in the two groups of mafic magmatic rocks (DSP and DBSC) in the study area. Figured blue: dolerites from the Pan-African basement (DSP) and figured red: dolerites from the Cretaceous sedimentary basins (DBSC).

The Harkers diagrams for the major elements show a decreasing pattern for the elements Fe_2O_3, TiO_2 P_2O_5, K_2O and MnO as SiO_2 increases (**Figure 4**). The decreasing profile of oxide contents is the cause of fractionation of mafic minerals such as clinopyroxenes and opaques. Alumina presents a variable profile in DSP and slightly decreasing in DBSC. The CaO, MgO and Na_2O contents increase as the SiO_2 content increases. The decrease in the P_2O_5 content in the DBSC and DSP as a function of silica could reflect the circulation of hydrothermal fluids. In these Harker plots, the PletM2 sample deviates from the profiles.

✓ **Behaviors of trace elements**

The diagrams of trace elements versus silica (**Figure 5**) generally show a decreasing evolution in the two groups of rocks. The contents of trace elements such as Nb, Y, Ce, Zr, Ba, and Sr decrease with the increase in the SiO_2 content, however the Ni and Sc contents show an increasing rate as the content increases in SiO_2 increases.

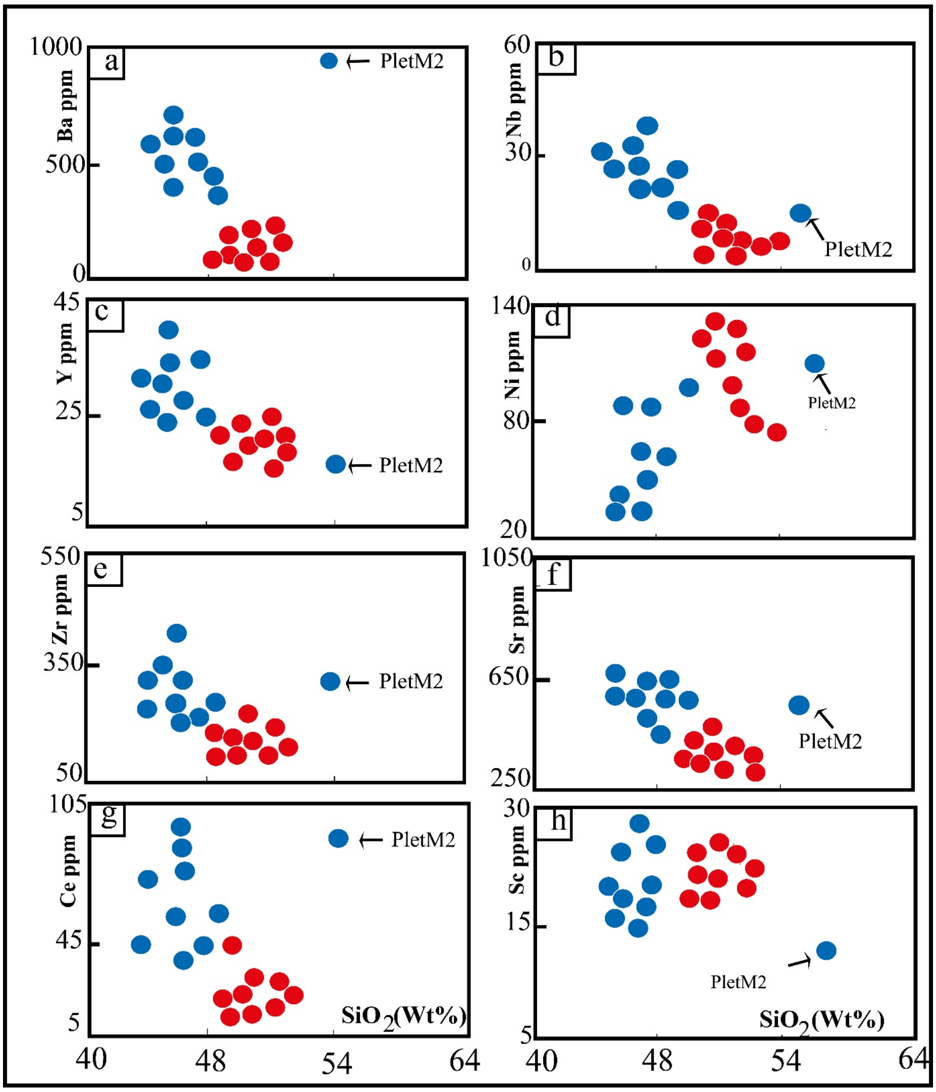

Figure 5. Harker type evolution diagrams showing the variation of trace elements in the two groups of dolerites in the study area. Figured blue: dolerites from the Pan-African basement (DSP) and figured red: dolerites from the Cretaceous sedimentary basins (DBSC).

5. Rare Earth Spectra and Multi-Element Diagrams

5.1. Hypovolcanic Rocks of the Pan-African Basement (DSP)

The rare earth spectra normalized to chondrites (Mc Donough and Sun, 1995) 25 (Figure 6) of the DSP are marked by the fractionation of light rare earths compared to heavy rare earths ((La/Yb) N = 8.24 - 25.24). The sum of rare earths (ΣREE) varies from 100.85 to 252.23 ppm. The HREE ratio is 1.64 ≤ (Gd/Yb)N ≤ 3.65. The negative anomaly in Europium is weak (0.8 ≤ Eu/Eu* ≤ 1.

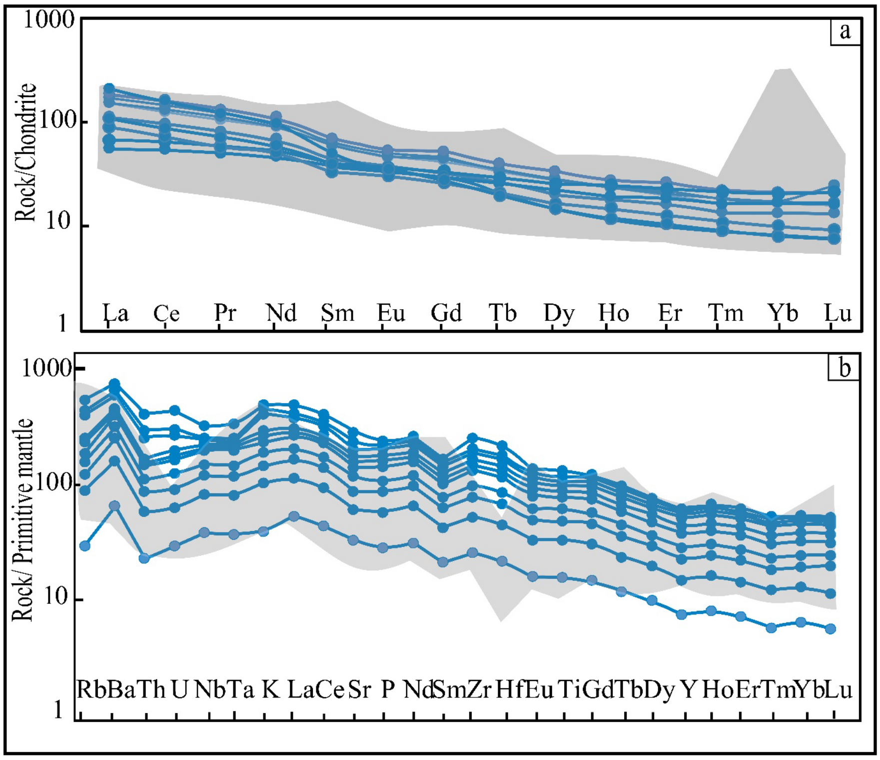

Figure 6. Rare earth spectra and multi-element diagrams of hypovolcanic rocks from Cretaceous sedimentary basins (a, b), normalized to chondrites [25] and the Primitive Mantle [26]. The gray part represents the dolerites of Mayo Oulo-Léré [27], Biden [28], MAM, Kendem, Dschang, Bangoua and Banganté [29], Banganté, Dschang and Manjo [30], Bamwa [31], Mongo [32] and Mbaoussi [33] which are studied in the other localities.

The DSP are therefore not the product of the fractional crystallization of a basaltic precursor, the dominant process in the establishment of calc-alkaline magmas with similar SiO_2 contents (43.85% - 55.87%) in the zones of current subduction.

Multielement spectra normalized to the primitive mantle (Sun and Mc Donough, 1989) for the DSPs (**Figure 7**) show negative anomalies in Sm, Eu and Ta and positive anomalies in Ba, U, La, Zr and Hf. They also present an enrichment in incompatible LILE type elements (Rb, Ba, Th) compared to incompatible HFSE type elements (Dy, Y, Yb). These characteristics are associated with calc-alkaline magmas that are formed in subduction zones. They result from the enrichment of the source mantle of these magmas by fluids.

The DSPs present rare earth spectra normalized to chondrites and multielement profiles normalized to the primitive mantle with negative slope, an enrichment in LILE and HFSE relative to the primitive mantle (**Figure 6(a)** and **Figure 6(b)**) comparable to those of the hypovolcanic formations of other localities of Cameroon and Chad described. These comparison dolerites have weak negative Eu anomalies at Mayo Oulo-Léré (Eu/Eu* = 0.37), Banganté (Eu/Eu* = 0.26); of Biden (Eu/Eu* = 0); Mbaoussi (Eu/Eu* = 0.36); Mongo (Eu/Eu* = 0.26) and Ntem (Eu/Eu* = 0.34). These dolerites are characterized by a very low enrichment in

MREE and HREE (1.01 ≤ $(Gd/Yb)_N$ ≤ 1.76). The DSP spectra are substantially parallel to those of dolerites from Mayo-Oulo, Banganté, Biden, Mbaoussi and Mongo. These characters also suggest that DSPs have a tholeiitic affinity.

5.2. Hypovolcanic Rocks of Cretaceous Sedimentary Basins (DBSC)

The rare earth spectra normalized to DSBC chondrites attest to the low fractionation of rare earths (ΣREE = 45.95 - 130.32 ppm). They also show a regular negative slope characterized by a low enrichment in LREE ($(La/Yb)_N$ = 2.87 - 4.20) similar to the fractionation of HREE ($(Gd/Yb)_N$ = 2.13 - 5.36). These DBSCs do not have a negative Europium anomaly (Eu/Eu* = 1).

The multielement spectra normalized to the primitive mantle (**Figure 7(b)**) of DBSC show a strongly negative slope characterized by a strong enrichment in LILE (Rb, Ba, Th) compared to HFSE (Dy, Y, Yb). These multielement spectra present negative anomalies in Rb, Th, Ce, P, Sm, Y, and Tm and positive anomalies in Ba, U, La, Zr, Hf. The positive anomalies in Ba, Sr, Ti and Ta are compatible with the accumulation of plagioclase.

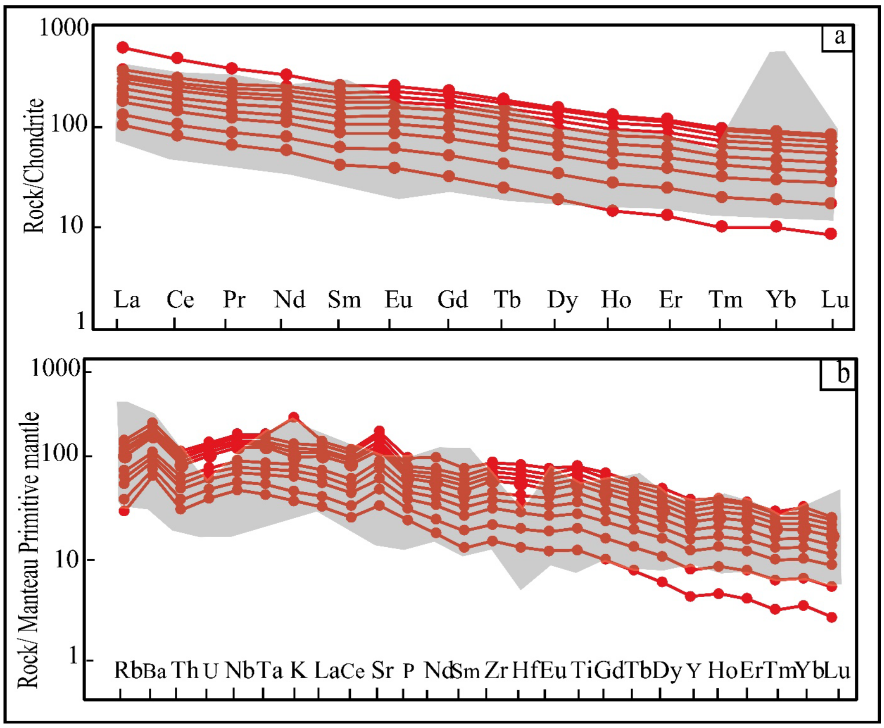

Figure 7. Rare earth spectra and multi-element diagrams of hypovolcanic rocks from Cretaceous sedimentary basins (a, b), normalized to chondrites [25] and the Primitive Mantle [26]. The gray part represents the dolerites of Mayo Oulo-Léré [27], Biden [28], MAM, Kendem, Dschang, Bangoua and Banganté [29], Banganté, Dschang and Manjo [30], Bamwa [31], Mongo [32] and Mbaoussi [33] which are studied in the other localities.

Depending on the behavior of rare earth $(La/Sm)_N$ (**Figure 8(a)** and **Figure 8(b)**), two groups of rocks are distinguished: DSPs (1.48 - 4.14) and DBSCs (1.23 - 2.46). These two groups of mafic hypovolcanic rocks are also distinguished by the contents of P_2O_5, Zr, Hf, Ba, Sr and Th which are relatively higher in the DSPs than those contained in the DBSCs.

6. Discussion

6.1. Geochemical Characters of Hypovolcanic Formations

6.1.1. Petrogenesis: Partial Fusion-Origin

Undersaturated alkaline magmas rich in volatile elements are markers of the important role of fluids in the mantle and of fluid-rock and magma-rock interactions, key processes for understanding the dynamics of the convective mantle and asthenosphere-lithosphere interactions in the intracontinental domain [34]. REEs were chosen because their behavior during fusion processes produces smooth spectra on the chondrite-normalized diagrams. The spectra provide information on partial fusion rates, with REE enrichment being inversely proportional to the fusion rate [35]-[38]. Also, they make it possible to determine the fusion process involved. DSPs are characterized by a preferential enrichment in LILE compared to HFSE and negative Nb-Ta anomalies. Extremely high Rb/Sr ratios generally cannot result in the partial melting that would involve typical crustal rocks thereby reflecting Rayleigh fractionation [39]. Studies have suggested that partial melting of the granulites constituting the Pan-African basement would result in magmas with very low Rb/Sr ratios in agreement with the low average (0.023) of the granulites of Taylor and McLeman [40]. Such weak ratios, although quite close to the average of the reference granulites, are not observed in the hypovolcanic formations of Figuil-Léré where the Rb/Sr ratio varies from 0.027 to 0.081 (avg: 0.054) in the DSP and from 0.017 at 0.067 (avg: 0.028) in DBSCs. These reports would be proof that the hypovolcanic formations studied do not come from the partial fusion of granitoids from the Pan-African basement (Rb/Sr: 1.29 - 30.13; [41] [42] but rather they are of mantle origin. In addition, the fact that the ratios of incompatible elements particularly LILE/HFSE (Rb/Nb, Rb/Zr) are higher in the Pan-African basement granitoids (Rb/Nb: 2.34 - 11.54 and Rb/Zr: 0.50 - 2.39; de Figuil-Léré (Rb/Nb: 0.51 - 3.45; Rb/Zr: 0.046 - 0.36 [36]-[38]. corroborates with this hypothesis according to which the hypovolcanic formations are not resulting from the partial fusion of granitoids.

6.1.2. Fractional Crystallization

Compared to the primitive magmas of the mantle, the very variable contents of MgO, Mg# (32.8 - 62.6) and transition elements (Sc, Cr, Co, Ni) of the mafic hypovolcanic rocks studied suggest that a certain degree of fractional crystallization occurred during the emplacement of mafic hypovolcanic rocks [16]. The mafic hypovolcanic rocks studied are rocks of basaltic and homogeneous composition ($43.83 < SiO_2 < 55.87\%$; $7.13 < Fe_2O_3 < 16.83\%$; $4.07 < MgO < 7.41\%$; $1.21 < TiO_2 < 4.48\%$; $Al_2O_3 < 18$ and $2.73 < Na_2O + K_2O < 7.63$. Such an evolution, typical of tholeiitic magmas, reflects a crystallization of the oxides as suggested by the textural relationships [36]-[38] [43] [44]. Arth [45] inside the magma chamber or during their ascent towards the surface of the earth's crust. The magmas, rising towards the surface, would have evolved by fractional crystallization while assimilating part of the continental crust, that is to say by the process known as AFC (assimilation coupled with fractional crystallization [36]-[38] [46] (**Figure 8(a)**). The AFC phenomenon makes it possible to explain the presence of fine-grained gabbros between the dolerites, of two groups of dolerites in the Figuil-Léré area (**Figure 8(a)**), of the gap in chemical composition observed between the basic rocks /intermediate and advanced.

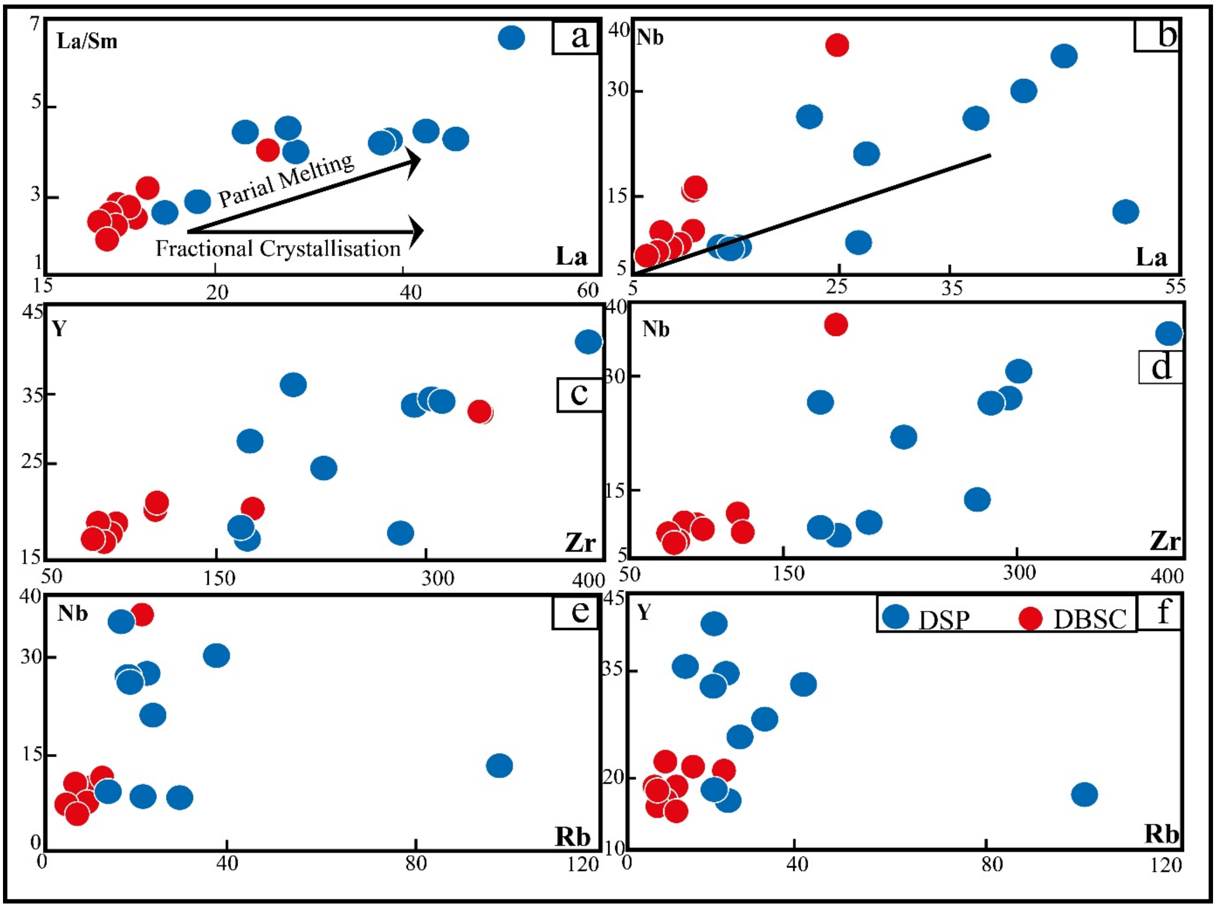

Figure 8. Diagrams illustrating partial melting and fractional crystallization. (a-f) Diagrams of variation of trace elements as a function of La, Zr and Rb in the dolerites of the study area. Figured blue: dolerites from the Pan-African basement (DSP) and figured red: dolerites from the Cretaceous sedimentary basins (DBSC).

The behavior of trace elements in these different diagrams is a principle allowing us to show that the hypovolcanic formations of Figuil - Léré display an evolution dominated by fractional crystallization from dolerites to fine-grained gabbros. These correlations indicate that the magmas at the origin of the hypovolcanic formations probably came from the same source. The collinearities of trace element variations shown by the different diagrams (**Figure 8**) also indicate the probable development of fractional crystallization processes operating in more or less enriched and/or contaminated mantello-derived magmas [36]-[38].

6.2. Crustal Contamination

The Th/Yb vs Ta/Yb diagram demonstrates the organization of the samples into two groups of rocks following the fractional crystallization process which was probably coupled with slight crustal contamination in the DSPs compared to that contained in the DBSCs (**Figure 9(a)**). These processes have also been described in other continental tholeiites by several authors [36]-[38] [47]-[50]. Based on this hypothesis, [51] [52] showed in the Rb/Y vs Nb/Y diagram that the Decan lavas in India were divided into two groups including a group contaminated with high Rb/Y ratios and low and relatively constant Nb/Y ratios, and another uncontaminated group defining a positive slope.

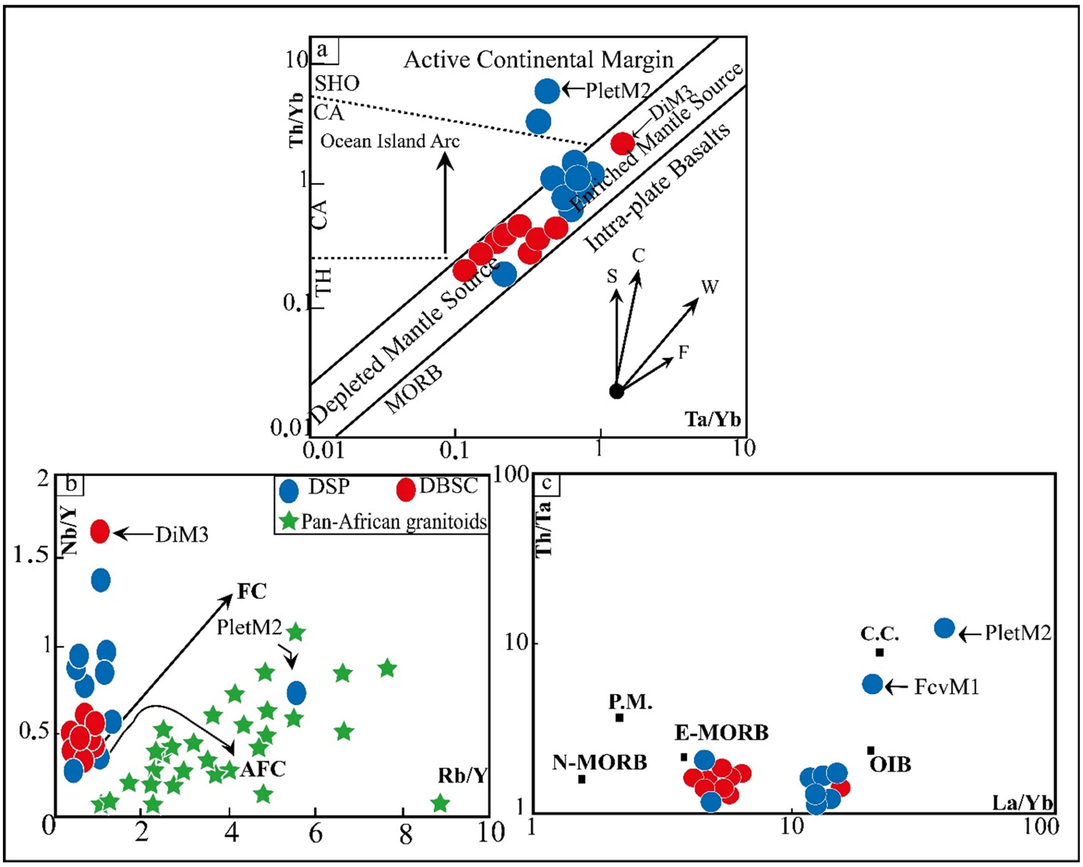

Figure 9. Diagrams illustrating the crustal contamination of the hypovolcanic rocks of Figuil and Léré. (a) diagram of Th/Yb vs Ta/Yb ratios applied to the two groups of rocks in the Léré-Figuil sector; CA: calc-alkaline, SHO: shoshonite, TH: tholeiitic basalts. The vectors S, C, W and F referring to the subduction zone, crustal contamination, intraplate fractionation and fractional crystallization respectively according to Pearce [53], (b) Diagram of Nb/Y vs Rb/Y according to Cox and Hawkesworth [52] and Leeman and Hawkesworth [56] showing the position of Pan-African granitoids in relation to that of dolerites. Data for Pan-African granitoids are from [41] [42] and [54]. CF: fractional crystallization; ACF: fractional assimilation-crystallization, (c) Position of the Figuil and Léré rocks in the Th/Ta vs La/Yb diagram [54]; OIB, E-MORB, N-MORB and PM according to Sun and McDonough [26], C. C: continental crust, according to Taylor and McLennan [40].

The hypovolcanic formations of Figuil-Léré are located in the range of uncontaminated lavas, further from the granitoid domain of the Pan-African basement.

They appear to have a similar positive correlation to uncontaminated lavas (**Figure 9(b)**). Except for the PletM2 sample which is found in the field of Pan-African basement granitoids. This position of the PletM2 sample demonstrates that this sample would truly be contaminated by granitoids from the Pan-African basement [36]-[38].

The negative Nb anomaly, specific to subduction zone magmas, unrelated to that of Zr, suggests crustal contamination of a mantle basaltic magma in a context far from the influence of a subduction zone [56]. The continental crust has a low value of the Nb/U ratio (4.4 - 25) and high values of the La/Nb ratios (1.6 - 2.6) and Th/Nb (0.24 - 0.88). According to Rudnick and Gao (2003). Oceanic island basalts (OIB) and mid-oceanic ridge basalts (E-MORB and N-MORB) have high values of the Nb/U ratio (>45) and low values of the La/Nb ratio (0.8 - 1.1) and Th/Nb (<0.1) [26] [36]-[38] [57] [58]. While the hypovolcanic formations of Figuil-Léré present Nb/U (28.33 - 47.00), La/Nb (0.65 - 1.55), and Th/Nb (0.06 - 0.10) ratios similar to those of MORB and OIB, these values found in the rocks studied show a slight intervention or not of a crustal component during their genesis. The enrichment in LILE and LREE compared to enriched MORBs (E-MORB) and OIBs would result from the effect of crustal contamination [36]-[38] [59] [60]. The analogy of the dolerites in the study area with the hypovolcanic formations studied in other localities and the intervention of the crustal contamination process are also well illustrated by the Th/Ta vs La/Yb diagram of Condie [55] (**Figure 9(c)**). The representative points of the rocks are spread between the E-MORBs and the OIBs.

6.3. Source Characterization

In the TAS diagram (**Figure 4(b)**), the studied dolerites produce slightly alkaline (DSP) and sub-alkaline (DBSC) affinities. These dolerites present an original chemical signature as in the alkaline province of the Cameroon Line [28] [36]-[38]. This chemical signature qualifies them as CFB (Continental Flood Basalt) type tholeiites, poor in TiO_2 and typically of lithospheric origin [28]. The low TiO_2 content (1.28% - 3.44%) classifies the rocks studied in the series of continental tholeiite with a low proportion of oxides like that described in West Africa [61] in the CAMP in the southwest of Algeria [62] and also in the typical alkaline rocks of Miocene age of Ngaoundéré (3% - 4.6%; [63]).

The La vs La/Sm diagram (**Figure 9(a)**) demonstrates that the mafic rocks studied come from the partial melting of the same source and not from the fractional crystallization of a common magma. The high concentrations of Ba, Th and the presence of mineral phases rich in volatiles (hornblende) in certain rocks studied indicate the occurrence of mantle metasomatism during their magmatic genesis [27] [36]-[38]. The enrichment in LILE and LREE, characteristic of continental tholeiite, is interpreted either as the effect of a crustal contamination process [35] [37] [38] [50] [59], or as a characteristic of the mantle source [64] [65]. In the case of continental tholeiites from the study area, the ratios of incompatible elements are in favor of their origin from an enriched source such as those of enriched MORB (E-MORB) and OIB (**Figure 10(c)**). Indeed, the ratio (La/Ce) N > 1 (1.01 - 1.32) for the majority of samples and the ratio Zr/Nb < 20 (8.95 - 20.55) clearly indicate an enriched source [25] [66].

7. Geotectonic Context of the Mafic Hypovolcanic Rocks of Figuil-Léré

Geochemical Characteristics of Major Elements

DBSCs have a tholeiitic composition, with a Th/Ta ratio of between 1.2 and 12; similar to continental tholeiites but they present a relative enrichment in Nb characteristic of most initial rift tholeiites, partly of lithospheric origin. The chemical composition of dolerites is therefore original with low Nb-Ta anomalies. This notion differs from continental tholeiite, whose more moderate negative Nb-Ta anomalies are attributed to crustal contamination of magmas rising towards the surface. The DSPs and DBSs show an affinity with rocks of the tholeiitic series so the Figuil and Léré dolerites resemble other dolerites described as continental tholeiites in Cameroon, for example at Dschang, Bangangté and Manjo [30] Biden [28]; Mbaoussi [35]; Bafoussam [67] and Mayo Oulo-Léré [27].

8. Geotectonic Relationship

The Zr/4-Y-2Nb from Meschede [68] diagram (**Figure 10(a)**) shows that most of the DSP rocks and a sample of DBSC are plotted in the intraplate alkaline basalt

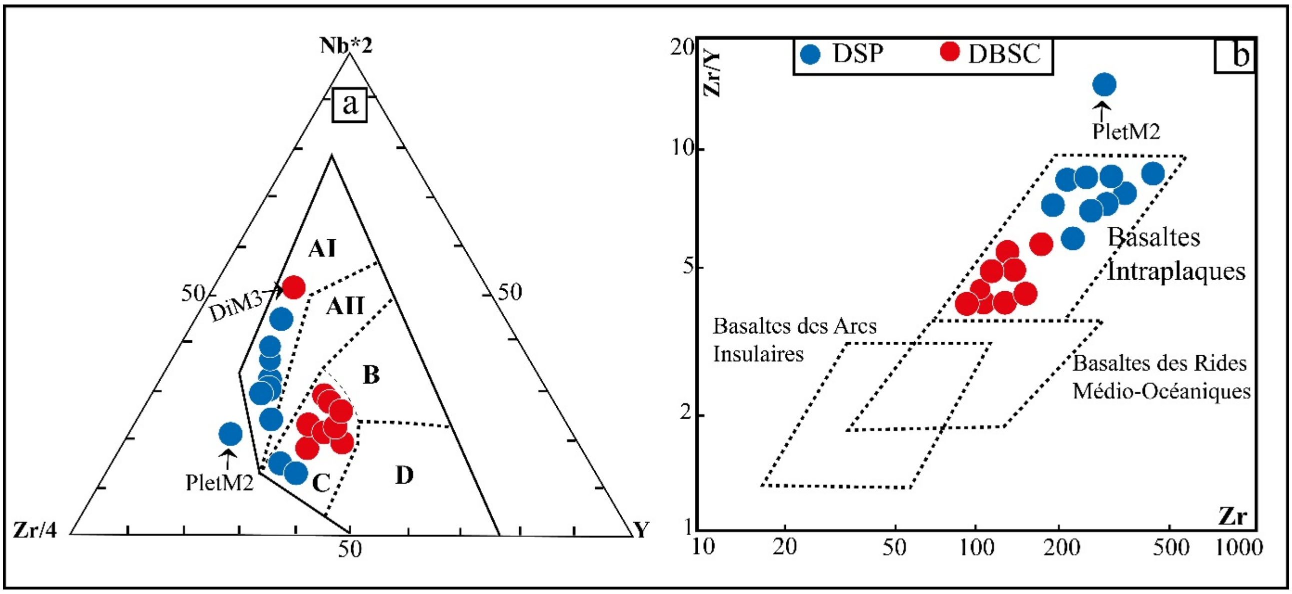

Figure 10. Diagrams illustrating the geodynamic context of the hypovolcanic formations of Figuil and Léré. (a) Ternary diagram of Zr/4-2Nb-Y from Meschede [68] showing the geotectonic context of the mafic magmatic rocks of the Cretaceous sedimentary basins of Figuil - Léré. AI: intraplate alkaline basalts (WPA); AII: intraplate tholeiitic basalts (WPT); B: P-type mid-ocean ridge basalts (P-MORB), C: Volcanic arc basalts (VAB), D: N-type mid-ocean ridge basalts (N-MORB), (b) Zr diagram/Y vs Zr of basaltic rocks [70] showing the location of mafic magmatic rocks studied in the area of intraplate basalts. Figured blue: dolerites from the Pan-African basement (DSP) and figured red: dolerites from the Cretaceous sedimentary basins (DBSC).

(AI) field. The majority of DBSC samples and two DSP samples are found in the range of volcanic arc basalts (C). The distribution of rocks in the field of intraplate alkaline basalts (AI) and volcanic arc basalts (C) without reaching the other domains (AII, B or D) suggests that the DSCs and the DBSCs are assigned to a orogenic magmatism because of their poverty in Ti and Na of pyroxenes [69].

The negative Nb, Ta and Ti anomalies in the hypovolcanic rocks of Figuil and Léré are interpreted as the imprints of older magmatism linked to subduction [36]-[38] [71]. This approach makes it possible to suggest a geotectonic context of active continental margin linked to a subduction system for the dolerites. On the binary diagram Zr/Y vs Zr of Pearce [70] (**Figure 10(b)**) used for the discrimination of the geodynamic context of basaltic rocks, the rocks studied generally fall into the domain of intraplate alkaline basalts characterized by a content of Zr quite high. These characteristics differentiate them from MORBs and island arc basalts by the relatively high Zr/Y ratio. This demonstrates that the mafic rocks would have formed in a single context. On the other hand, the PletM2 sample cannot be classified in the two diagrams (**Figure 10(a)** and **Figure 10(b)**).

9. Geodynamic Relationships in Ternary Diagrams

Y/15-La/10-Nb/8 and (TiO_2-MnO*10-P_2O_5*10)

The magmatic evolution of the Figuil-Léré zone is suggested by a $(Nb/La)_N$ ratio between 0.25 and 0.89 in the DSP similar to that of the source basalts while the (Nb/La) ratio N ranges from 1 to 1.49 in DBSCs. The DSPs were set up along Pan-African faults that could mark extensive stresses linked to post-rift transpression which affected the Cenomanian belt of Central Africa [36]-[38] [72] from the Upper Santonian. The Y/15-La/10-Nb/8 diagram (**Figure 11(a)**) of Cabanis and Lecolle [44] shows that the two (2) DSP samples fall within the orogenic (compressive) field. Just as the dolerites of Biden (3 samples), Bamwa (2 samples), Mongo (1 sample) and Mbaoussi (1 sample) are placed in the orogenic (compressive) field unlike the majority of dolerite samples from Manjo, Dschang, Banganté, Kendem, MAM, Mayo-Oulo, Ntem and certain samples from Mbaoussi, Bamwa and Mongo which occupy the intracontinental field late in post-orogenic (compressive to distensive). However, the majority of DSP samples, 3 DBSC samples are found in the late to post-orogenic intracontinental dominant (compressive to distensive).

The diagram (**Figure 11(b)**) (TiO_2-MnO*10-P_2O_5*10) of Muller [73] is used to differentiate the different magmatic series and geodynamic environments, that is to say it allows to replace magmatic series in different geodynamic contexts. In this research study, the majority of dolerites studied in other localities in Cameroon and a sample of DSP are found in the island arc tholeiites (IAT) field [36]-[38]. On the other hand, 3 DBSC samples associated with those of DSP are placed in the domain of oceanic island basalts as are certain samples from Bamwa, Mongo, Manjo, Biden, Mayo-oulo, Mbaoussi and Banganté. While in the field of MORB the DBSCs are plotted.

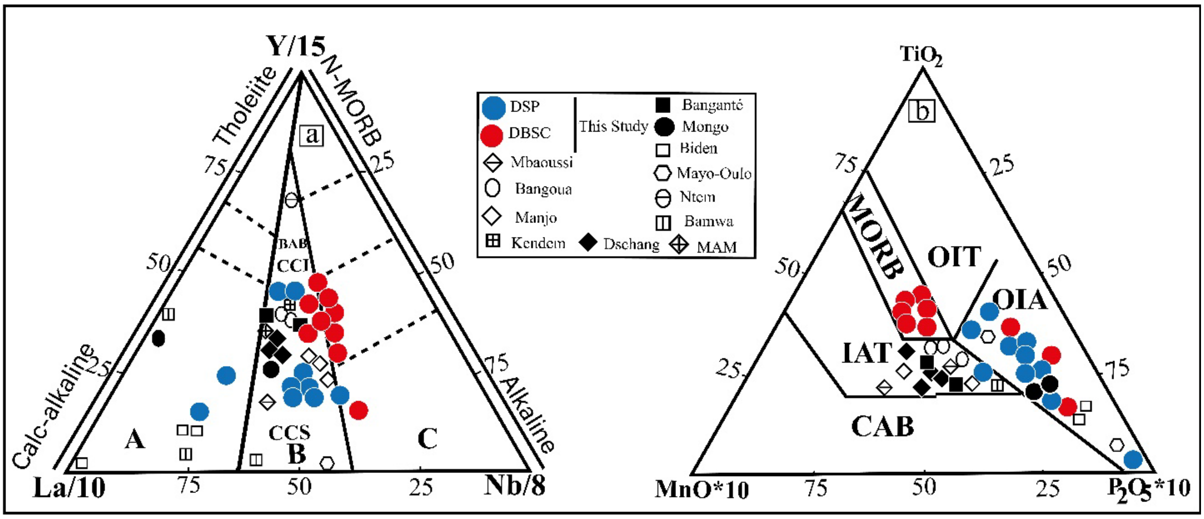

Figure 11. Diagrams illustrating the comparative study in the geodynamic context. (a) Diagram Y/15-La/10-Nb/8 of Cabanis and Lecolle [44], BAB: back-arc basin basalts, CCI: lower continental crust, CCS: upper continental crust, A: orogenic domain (compressive), B: late to post-orogenic intracontinental domain (compressive to distensive), or intermediate domain of continental tholeiites (TC) and basin basalts back-arc (BAB), C: non-orogenic (distensive) domain of ridge tholeiites and intra-plate alkaline basalts, (b) Position of the Léré and Figuil rocks in Muller's TiO_2-MnO-P_2O_5 diagram [73], IOT: tholeiites from oceanic islands, OIA: alkaline basalts from oceanic islands, CAB: basalts calc-alkaline, IAT: island arc tholeiites and MORB: mid-oceanic ridge basalts. The gray part represents the dolerites of Mayo Oulo-Léré [27] [28], MAM, Kendem, Dschang, Bangoua and Banganté [29], Banganté, Dschang and Manjo [30], Bamwa [31], Mongo [32] and Mbaoussi [33] which are studied in other localities. Figured blue: dolerites from the Pan-African basement (DSP) and Figured red: dolerites from the Cretaceous sedimentary basins (DBSC).

In short, the difference in the mode of distribution of the rocks studied in the field does not necessarily suggest the establishment of a distinct magmatic suite. Indeed, these variations may be due to differences in the setting environment, for example, the injection into the Pan-African basement will be influenced among other things by the presence of networks of fractures and faults. The correlations between the different oxides and the silica content highlight the important role of partial melting and fractional crystallization processes in the evolution of these mafic hypovolcanic rocks.

The magma at the origin of the dolerites studied derives from the fusion of a depleted mantle or an enriched mantle with a low partial melting rate. The high LILE contents could be indicative of either a mantle source and/or crustal contamination. We can envisage, for Figuil-Léré magmatism, a process of fractional crystallization of a transitional basaltic magma, which would produce the basic to intermediate series, coupled with an assimilation of continental crust.

10. Conclusion

The geochemical study of mafic hypovolcanic magmatic rocks confirms the ultrabasic, basic, intermediate and also differentiated characters ($43.83 < SiO_2 < 55.85\%$). The DSPs are placed in the alkaline field, whereas the DBSCs occupy the sub-alkaline zone. All the facies (dolerites and fine-grained gabbros) up to the trachytes form a transitional suite, characterized by TiO_2 (low) and P_2O_5 (medium). The tholeiitic character with alkaline affinity suggests the transition between alkaline magmatism and tholeiitic magmatism. The existence of two tholeiitic families with alkaline affinity deserves to be highlighted among fine-grained dolerites and gabbros. The synchronous presence of tholeiitic and alkaline magmatism has been reported in numerous environments including the Afar continental rift and the Hainan Island in South China. The magmatism of the study area is characterized by the process of fractional crystallization coupled with the assimilation of continental crust thus producing the basic and intermediate series. Except for the PletM2 sample which was found in a different position in the granitoid field, this shows that it would really be contaminated by granitoids from the Pan-African basement. The dolerites studied would come from the same parental magma as shown by the ratios Zr/Hf: 37.56 - 43.08 and Nb/Ta: 15.16 - 19.60 of the DSP and Zr/Hf: 34.34 - 46.48 and Nb/Ta 14.34 - 19.31 of DBSCs which are substantially identical. This hypothesis suggests the presence of a single magma: alkaline magma coming from a deep source.

Conflicts of Interest

The authors declare no conflicts of interest regarding the publication of this paper.

References

[1] Srivastava, R.K. (2011) Dyke Swarms: Keys for Geodynamic Interpretation. Springer.

[2] Halls, H.C. (1987) Introduction. In: Halls, H.C. and Fahrig, W.F., Eds., *Mafic Dyke Swarms*, Geological Association of Canada, 1-3.

[3] Bouyo, H.M., Zhao, Y, Penaye, J., Zhang, S.H. and Njel, U.O. (2015) Roches métavolcaniques et métasédimentaires liées à la subduction néoprotérozoïque de la ceinture de roches vertes de Rey Bouba au centre-nord du Cameroun en Afrique Centrale, Precambrien Research. Elsevier.

[4] Maurin, J.-C. and Guiraud, R. (1990) Relationships between Tectonics and Sedimentation in the Barremo-Aptian Intracontinental Basins of Northern Cameroon. *Journal of African Earth Sciences* (*and the Middle East*), **10**, 331-340. https://doi.org/10.1016/0899-5362(90)90064-l

[5] Maurin, J. and Guiraud, R. (1993) Basement Control in the Development of the Early Cretaceous West and Central African Rift System. *Tectonophysics*, **228**, 81-95. https://doi.org/10.1016/0040-1951(93)90215-6

[6] Bessoles, B. and Trompette, R. (1980) La chaîne panafricaine. Zone mobile d'Afrique Centrale (partie sud) et zone soudanaise. *Mémoire du Bureau de Recherches Géologiques et Minières*, **92**, 394.

[7] Oliveira, E.P., Toteu, S.F., Araújo, M.N.C., Carvalho, M.J., Nascimento, R.S., Bueno, J.F., *et al.* (2006) Geologic Correlation between the Neoproterozoic Sergipano Belt (NE Brazil) and the Yaoundé Belt (Cameroon, Africa). *Journal of African Earth Sciences*, **44**, 470-478. https://doi.org/10.1016/j.jafrearsci.2005.11.014

[8] van Schmus, W.R., Oliveira, E.P., da Silva Filho, A.F., Toteu, S.F., Penaye, J. and Guimarães, I.P. (2008) Proterozoic Links between the Borborema Province, NE Brazil, and the Central African Fold Belt. *Geological Society*, *London*, *Special Publications*, **294**, 69-99. https://doi.org/10.1144/sp294.5

[9] Fosso Menkem, E. (2018) Tectonic-Sedimentary Evolution and Paleo-Environments

of the Cretaceous Babouri-Figuil and Mayo-Oulo-Léré basins (North Cameroon). University of Yaoundé.

[10] Penaye, J., Kröner, A., Toteu, S.F., Van Schmus, W.R. and Doumnang, J. (2006) Evolution of the Mayo Kebbi Region as Revealed by Zircon Dating: An Early (Ca. 740Ma) Pan-African Magmatic Arc in Southwestern Chad. *Journal of African Earth Sciences*, **44**, 530-542. https://doi.org/10.1016/j.jafrearsci.2005.11.018

[11] Kasser, M.Y. (1995) Precambrian Evolution of the Mayo-Kebbi Region. A Segment of the Pan-African Channel. Thesis National Museum of Natural History of Paris.

[12] Dejax, J. and Brunet, M. (1996) The Fossil Floras of the Hamakoussou Basin, Lower Cretaceous of Northern Cameroon: Biostratigraphic Correlations with the Benue Trench, Paleogeographical Implications. *Bulletin des Centres de Recherches Exploration-Production Elf-Aquitaine*, **16**, 145-173.

[13] Dawaï, D. (2014) The Guider and Bossoum-Pologozom plutons (Pan-African Range in Northern Cameroon): Petrographic, Structural, Magnetic and Geochronological Analysis and Geodynamic Implication. Doctoral Thesis, University of Toulouse.

[14] Schwoerer, P. (1965) Geological Reconnaissance Map at the Scale of 1:500,000 and Explanatory Notice on the Garoua-Est Sheet.

[15] Ndjeng, E. (1992) Geodynamic Evolution Model of Two Lower Cretaceous Basins of North Cameroon: Babouri-Figuil and Mayo Oulo-Léré. University of Yaoundé.

[16] Frey, F.A., Green, D.H. And Roy, S.D. (1978) Integrated Models of Basalt Petrogenesis: A Study of Quartz Tholeiites to Olivine Melilitites from South Eastern Australia Utilizing Geochemical and Experimental Petrological Data. *Journal of Petrology*, **19**, 463-513. https://doi.org/10.1093/petrology/19.3.463

[17] Bas, M.J.L., Maitre, R.W.L., Streckeisen, A. And Zanettin, B. (1986) A Chemical Classification of Volcanic Rocks Based on the Total Alkali-Silica Diagram. *Journal of Petrology*, **27**, 745-750. https://doi.org/10.1093/petrology/27.3.745

[18] Le Maître, R.W. (2002) Igneous Rocks. A Classification and Glossary of Terms. Recommendations of the International Union of Geological Sciences Sub Commission on the Systematics of Igneous Rocks. Cambridge University Press.

[19] Miyashiro, A. (1974) Volcanic Rock Series in Island Arcs and Active Continental Margins. *American Journal of Science*, **274**, 321-355. https://doi.org/10.2475/ajs.274.4.321

[20] Winchester, J.A. and Floyd, P.A. (1976) Geochemical Magma Type Discrimination: Application to Altered and Metamorphosed Basic Igneous Rocks. *Earth and Planetary Science Letters*, **28**, 459-469. https://doi.org/10.1016/0012-821x(76)90207-7

[21] Pearce, J.A. (1996) A User's Guide to Basalt Discrimination Diagrams. Trace Element Geochemistry of Volcanic Rocks: Application for Massive Sulphide Exploration. *Geological Association of Canada*, *Short Course Notes*, **12**, 79-113.

[22] Floyd, P.A. and Winchester, J.A. (1975) Magma Type and Tectonic Setting Discrimination Using Immobile Elements. *Earth and Planetary Science Letters*, **27**, 211-218. https://doi.org/10.1016/0012-821x(75)90031-x

[23] Pearce, J.A. (1975) Basalt Geochemistry Used to Investigate Past Tectonic Environments on Cyprus. *Tectonophysics*, **25**, 41-67. https://doi.org/10.1016/0040-1951(75)90010-4

[24] Ould-Yahoui, A., Sbai, O., Baranger, K., Bernard, A., Gueye, Y., Charrat, E., *et al.* (2013) Role of Matrix Metalloproteinases in Migration and Neurotrophic Properties of Nasal Olfactory Stem and Ensheathing Cells. *Cell Transplantation*, **22**, 993-1010. https://doi.org/10.3727/096368912x657468

[25] McDonough, W.F. and Sun, S.-S. (1995) The Composition of the Earth. *Chemical Geology*, **120**, 223-253. https://doi.org/10.1016/0009-2541(94)00140-4

[26] Sun, S.-. and McDonough, W.F. (1989) Chemical and Isotopic Systematics of Oceanic Basalts: Implications for Mantle Composition and Processes. *Geological Society*, *London*, *Special Publications*, **42**, 313-345. https://doi.org/10.1144/gsl.sp.1989.042.01.19

[27] Ngounouno, I., Déruelle, B., Guiraud, R. and Vicat, J. (2001) Magmatismes tholéiitique et alcalin des demi-grabens crétacés de Mayo Oulo-Léré et de Babouri–Figuil (Nord du Cameroun-Sud du Tchad) en domaine d'extension continentale. *Comptes Rendus de l'Académie des Sciences—Series IIA—Earth and Planetary Science*, **333**, 201-207. https://doi.org/10.1016/s1251-8050(01)01626-3

[28] Vicat, J., Ngounouno, I. and Pouclet, A. (2001) Existence de dykes doléritiques anciens à composition de tholéiites continentales au sein de la province alcaline de la ligne du Cameroun. Implication sur le contexte géodynamique. *Comptes Rendus de l'Académie des Sciences—Series IIA—Earth and Planetary Science*, **332**, 243-249. https://doi.org/10.1016/s1251-8050(01)01526-9

[29] Tchouankoue, J.P., Simeni Wambo, N.A., Kagou Dongmo, A. and Li, X. (2014) ^{40}Ar/^{39}Ar Dating of Basaltic Dykes Swarm in Western Cameroon: Evidence of Late Paleozoic and Mesozoic Magmatism in the Corridor of the Cameroon Line. *Journal of African Earth Sciences*, **93**, 14-22. https://doi.org/10.1016/j.jafrearsci.2014.01.006

[30] Pierre Tchouankoue, J. (2012) Petrology, Geochemistry, and Geodynamic Implications of Basaltic Dyke Swarms from the Southern Continental Part of the Cameroon Volcanic Line, Central Africa. *The Open Geology Journal*, **6**, 72-84. https://doi.org/10.2174/1874262901206010072

[31] Nkouandou, O.F., Bardintzeff, J., Mahamat, O., Fagny Mefire, A. and Ganwa, A.A. (2017) The Dolerite Dyke Swarm of Mongo, Guéra Massif (Chad, Central Africa): Geological Setting, Petrography and Geochemistry. *Open Geosciences*, **9**, 138-150. https://doi.org/10.1515/geo-2017-0012

[32] Nkouandou, O.F., Ngounouno, I., Déruelle, B., Ohnenstetter, D., Montigny, R. and Demaiffe, D. (2007) Petrology of the Mio-Pliocene Volcanism to the North and East of Ngaoundéré (Adamawa, Cameroon). Comptes Rendus. *Géoscience*, **340**, 28-37. https://doi.org/10.1016/j.crte.2007.10.012

[33] Nkouandou, O., Bardintzeff, J., Dogsaye, P. and Mefire, A. (2016) Geochemistry and Petrogenesis of Mafic Doleritic Dykes at Mbaoussi (Adamawa Plateau, Cameroon, Central Africa). *Journal of Geography*, *Environment and Earth Science International*, **8**, 1-18. https://doi.org/10.9734/jgeesi/2016/28198

[34] Chamboredon, R. (2015) Characterization and Origin of Alkaline Magmas and Fluids under the Jbel Saghro Volcanic Massif, Anti Atlas, Morocco. Doctoral Thesis, University of Montpellier.

[35] Shaw, D.M. (1970) Trace Element Fractionation during Anatexis. *Geochimica et Cosmochimica Acta*, **34**, 237-243. https://doi.org/10.1016/0016-7037(70)90009-8

[36] Klamadji, M.N., Dedzo, M.G., Tchameni, R. and Dawaï, D. (2020) Petrography and Geochemical Characterization of Dolerites from Figuil (Northern Cameroon) and Léré (Southwestern Chad). *International Journal of Geosciences*, **11**, 459-482. https://doi.org/10.4236/ijg.2020.117023

[37] Klamadji, M.N. (2021) Petrology and Geochemistry of the Mafic Hypovolcanic Formations of Figuil (North Cameroon) and Lrée (Southwest Chad): Geodynamic Implication. University of Maroua.

[38] Klamadji, M.N., Dedzo, M.G., Tchameni, R., Hamadjoda, D.D., Nyotok, P.C.B.A. and Onana, G. (2021) Fractional Crystallization and Crustal Contamination of Doleritic

and Trachytic Dykes Crosscutting the Cretaceous Sedimentary Basins from Figuil (North Cameroon) and Léré (South-Western Chad): Geodynamic Implications. *Journal of Geoscience and Environment Protection*, **9**, 190-210. https://doi.org/10.4236/gep.2021.912012

[39] Halliday, A.N., Davidson, J.P., Hildreth, W. and Holden, P. (1991) Modelling the Petrogenesis of High Rb/Sr Silicic Magmas. *Chemical Geology*, **92**, 107-114. https://doi.org/10.1016/0009-2541(91)90051-r

[40] Taylor, S.R. and McLennan, S.M. (1985) The Continental Crust: It's Composition and Evolution. Blackwell Publications.

[41] Doumnang, J.C. (2006) The Geology of the Neoproterozoic Formations of Mayo-Kebbi (S-W Chad). Doctoral Thesis, University of Orléans.

[42] Isseini, M., André-Mayer, A., Vanderhaeghe, O., Barbey, P. and Deloule, E. (2012) A-type Granites from the Pan-African Orogenic Belt in South-Western Chad Constrained Using Geochemistry, Sr-Nd Isotopes and U-Pb Geochronology. *Lithos*, **153**, 39-52. https://doi.org/10.1016/j.lithos.2012.07.014

[43] Wager, L.R. and Deer, W.A. (1939) Olivines from the Skaergaard Intrusion, Kangerdlugssuak, East Greenland. *American Mineralogist*, **24**, 18-25.

[44] Cabanis, B. and Thieblemont, D. (1988) La discrimination des tholeiites continentales et des basaltes arriere-arc; Proposition d'un nouveau diagramme, le triangle Th-3xTb-2xTa. *Bulletin de la Société Géologique de France*, **6**, 927-935. https://doi.org/10.2113/gssgfbull.iv.6.927

[45] Arth, J.G. (1976) Behavior of Trace Elements during Magmatic Processes-Summary of Theoretical Models and Their Applications. *Journal of Research of the U.S. Geological Survey*, **4**, 41-47.

[46] DePaolo, D.J. (1981) Trace Element and Isotopic Effects of Combined Wall Rock Assimilation and Fractional Crystallisation, Earth Planet. *Science Letters*, **84**, 59-68.

[47] Marsh, J.S. (1989) Geochemical Constraints on Coupled Assimilation and Fractional Crystallization Involving Upper Crustal Compositions and Continental Tholeiitic Magma. *Earth and Planetary Science Letters*, **92**, 70-80. https://doi.org/10.1016/0012-821x(89)90021-6

[48] Valbracht, P.J., Helmers, H. and Beunk, F.F. (1991) Early Proterozoic Continental Tholeiites from Western Bergslagen, Central Sweden, I. Petrology, Geochemical Petrogenesis and Geotectonic Setting. *Precambrian Research*, **52**, 187-214. https://doi.org/10.1016/0301-9268(91)90080-t

[49] Cadman, A.C., Tarney, J., Bridgwater, D., Mengel, F., Whitehouse, M.J. and Windley, B.F. (2001) The Petrogenesis of the Kangâmiut Dyke Swarm, W. *Greenland. Precambrian Research*, **105**, 183-203. https://doi.org/10.1016/s0301-9268(00)00111-x

[50] Srivastava, R.K. and Singh, R.K. (2004) Trace Element Geochemistry and Genesis of Precambrian Sub-Alkaline Mafic Dikes from the Central Indian Craton: Evidence for Mantle Metasomatism. *Journal of Asian Earth Sciences*, **23**, 373-389. https://doi.org/10.1016/s1367-9120(03)00150-0

[51] Cox, K.G. and Hawkesworth, C.J. (1985) Relative Contribution of Crust and Mantle to Flood Basalt Magmatism, Mahabaleshwar, Deccan Traps. *Philosophic Transaction Royal Society London A*, **310**, 627-641.

[52] Leeman, W.P. and Hawkesworth, C.J. (1986) Open Magma Systems: Trace Element and Isotopic Constraints. *Journal of Geophysical Research*: *Solid Earth*, **91**, 5901-5912. https://doi.org/10.1029/jb091ib06p05901

[53] Pearce, J.A. (1982) Trace Elements Characteristics of Lavas from Destructive Plate Boundaries. Wiley.

[54] Nlomngan, J.P.S., Penaye, J., Tchameni, R., Owona, S., Ibohn, A.P.M., Nsifa, E.N., *et al.* (2019) Geochemical Characterization of Boula Ibi Granitoids and Implications in Geodynamic Evolution. *Journal of Geography and Geology*, **11**, 13. https://doi.org/10.5539/jgg.v11n4p13

[55] Condie, K.C. (1997) Sources of Proterozoic Mafic Dyke Swarms: Constraints from Thta and Layb Ratios. *Precambrian Research*, **81**, 3-14. https://doi.org/10.1016/s0301-9268(96)00020-4

[56] Touil, A., Bilal, E. and Boukhar, A.E. (2015) Distinction of Two Tholeiitic Families among the Late-Pan-African Dolerites of Siroua (Central Anti-Atlas, Morocco).

[57] Hofmann, A.W. (1988) Chemical Differentiation of the Earth: The Relationship between Mantle, Continental Crust, and Oceanic Crust. *Earth and Planetary Science Letters*, **90**, 297-314. https://doi.org/10.1016/0012-821x(88)90132-x

[58] Hollanda, M.H.B.M., Pimentel, M.M., Oliveira, D.C. and de Sá, E.F.J. (2006) Lithosphere-Asthenosphere Interaction and the Origin of Cretaceous Tholeiitic Magmatism in Northeastern Brazil: Sr-Nd-Pb Isotopic Evidence. *Lithos*, **86**, 34-49. https://doi.org/10.1016/j.lithos.2005.04.004

[59] Dostal, J., Baragar, W.R.A. and Dupuy, C. (1983) Geochemistry and Petrogenesis of Basaltic Rocks from Coppermine River Area, Northwest Territories. *Canadian Journal of Earth Sciences*, **20**, 684-698. https://doi.org/10.1139/e83-062

[60] Dupuy, C. and Dostal, J. (1984) Trace Element Geochemistry of Some Continental Tholeiites. *Earth and Planetary Science Letters*, **67**, 61-69. https://doi.org/10.1016/0012-821x(84)90038-4

[61] Marzoli, A., Bertrand, H., Knight, K.B., Cirilli, S., Buratti, N., Vérati, C., *et al.* (2004) Synchrony of the Central Atlantic Magmatic Province and the Triassic-Jurassic Boundary Climatic and Biotic Crisis. *Geology*, **32**, 973-976. https://doi.org/10.1130/g20652.1

[62] Chabou, M.C., Bertrand, H. and Sebaï, A. (2010) Geochemistry of the Central Atlantic Magmatic Province (CAMP) in South-Western Algeria. *Journal of African Earth Sciences*, **58**, 211-219. https://doi.org/10.1016/j.jafrearsci.2010.02.009

[63] Nkouandou, O.F., Ngounouno, I., Déruelle, B., Ohnenstetter, D., Montigny, R. and Demaiffe, D. (2007) Petrology of the Mio-Pliocene Volcanism to the North and East of Ngaoundéré (Adamawa, Cameroon). Comptes Rendus. *Géoscience*, **340**, 28-37. https://doi.org/10.1016/j.crte.2007.10.012

[64] Bertrand, H., Dostal, J. and Dupuy, C. (1982) Geochemistry of Early Mesozoic Tholeiites from Morocco. *Earth and Planetary Science Letters*, **58**, 225-239. https://doi.org/10.1016/0012-821x(82)90196-0

[65] Alibert, C. (1985) A Sr-Nd Isotope and REE Study of Late Triassic Dolerites from the Pyrenees (France) and the Messejana Dyke (Spain and Portugal). *Earth and Planetary Science Letters*, **73**, 81-90. https://doi.org/10.1016/0012-821x(85)90036-6

[66] Morata, D., Puga, E., Demant, A. and Aguirre, L. (1997) Geochemistry and Tectonic Setting of the «Ophites» from the External Zones Ofthe Betic Cordilleras (S. Spain). *Estudios Geológicos*, **53**, 107-120. https://doi.org/10.3989/egeol.97533-4236

[67] Nono, G.D.K., Wotchoko, P., Ganno, S., Njinchuki, D.N. and Nzenti, J.P. (2013) Petrochemical Characterization of Two Distinct Types of Dolerites from Bafoussam Area, West Cameroon. *International Journal of Geosciences*, **4**, 1131-1144. https://doi.org/10.4236/ijg.2013.48107

[68] Meschede, M. (1986) A Method of Discriminating between Different Types of Mid-Ocean Ridge Basalts and Continental Tholeiites with the Nb 1bZr 1bY Diagram. *Chemical Geology*, **56**, 207-218. https://doi.org/10.1016/0009-2541(86)90004-5

[69] Leterrier, J., Maury, R.C., Thonon, P., Girard, D. and Marchal, M. (1982) Clinopyroxene Composition as a Method of Identification of the Magmatic Affinities of Paleo-Volcanic Series. *Earth and Planetary Science Letters*, **59**, 139-154. https://doi.org/10.1016/0012-821x(82)90122-4

[70] Pearce, J.A. and Norry, M.J. (1979) Petrogenetic Implications of Ti, Zr, Y, and Nb Variations in Volcanic Rocks. *Contributions to Mineralogy and Petrology*, **69**, 33-47. https://doi.org/10.1007/bf00375192

[71] Kelemen, P.B., Shimizu, N. and Dunn, T. (1993) Relative Depletion of Niobium in Some Arc Magmas and the Continental Crust: Partitioning of K, Nb, La and Ce during Melt/Rock Reaction in the Upper Mantle. *Earth and Planetary Science Letters*, **120**, 111-134. https://doi.org/10.1016/0012-821x(93)90234-z

[72] Guiraud, R. and Maurin, J.C. (1991) Le Rifting en Afrique au Cretace inferieur; Synthese structurale, Mise en evidence de deux etapes dans la genese des bassins, Relations avec les ouvertures oceaniques peri-africaines. *Bulletin de la Société Géologique de France*, **162**, 811-823. https://doi.org/10.2113/gssgfbull.162.5.811

[73] Mullen (1983) MnO-TiO_2-P_2O_5 Diagram for Basaltic Samples from Khangai-Khentei Belt. The Samples Are Most Similar to Oceanic Island Alkaline Basalt. https://warmada.staff.ugm.ac.id/Graphics/gnuplot/petclass/mullen.html